고성능 형상 및 유리섬유/에폭시-우레탄 샌드위치 구조를 사용한 소형 풍력발전 블레이드의 공력 및 구조설계

공창덕* · 방조혁*

Aerodynamic and Structural Design on Small Wind Turbine Blade Using High Performance Configuration and E-Glass/Epoxy-Urethane Foam Sandwich Composite Structure

Chang-Duk Kong* · Jo-Hyug Bang*

ABSTRACT

This study proposes a development result for the 1-kW class small wind turbine system, which is applicable to relatively low wind speed regions like Korea and has the variable pitch control mechanism. In the aerodynamic design of the wind turbine blade, parametric studies were carried out to determine an optimum aerodynamic configuration which is not only more efficient at low wind speed but whose diameter is not much larger than similar class other blades. A light composite structure, which can endure effectively various loads, was newly designed. In order to evaluate the structural design of the composite blade, the structural analysis was performed by the finite element method. Moreover both structural safety and stability were verified through the full-scale structural test.

초 록

본 연구에서는 한국과 같이 비교적 저 풍속인 지역에 적용 가능하도록 피치제어장치를 가진 1kW 급 소형 풍력발전 시스템의 개발 결과를 제시하였다. 공력설계에서는 블레이드의 직경이 동급의 상용 블레이드 보다 과도하게 크지 않으면서도 저 풍속 지역에서 보다 효율적인 형상설계를 위해 여러 가지 설계 변수분석을 통한 파라미터 연구가 수행되었다. 또한 구조설계를 통해 풍력발전기에 작용하는 다양한 하중을 효과적으로 견딜 수 있는 경량의 복합재 구조가 설계되었다. 구조설계의 평가를 위해 유한요소 구조해석이 수행되었으며, 실물 구조시험을 수행하여 구조적 안전성을 확인하였다.

Key Words: Small Wind Turbine System(소형 풍력발전 시스템), Aerodyanmic Design & Analysis(공력설계 및 해석), Structural Design & Analysis(구조설계 및 해석), Structural Test(구조시험)

1. Introduction

Recently, the trend of the wind turbine system development has become much larger

† 2004년 3월 11일 접수 ~ 2004년 3월 18일 심사완료
* 정회원, 조선대학교 항공우주공학과
연락저자, E-mail: cdgong@chosun.ac.kr

scale over several MW classes. However, because the small-scale wind turbine system has some advantages, which someone can build personally it with low cost as well as experience the energy save effect, it has been continuously developed. Currently, because most commercialized small scale wind turbine systems have been designed with the rated wind speed more than 12m/s, they show great reduction of aerodynamic efficiency at the low wind speed region like Korea. In this design, a small-scale wind turbine blade, which not only can keep a proper blade length less than lengths of existing commercial products but also be acceptable for low wind speed region, was aerodynamically designed. A specific proper airfoil at low wind speed was selected, and the optimal aerodynamic design was derived through the parametric study on linear chord distribution and blade angle design with maximum lift-drag ratios. In structural design, the blade uses E-Glass/Epoxy composite and Urethane foam materials, and its structure adapts the skin/spar/foam sandwich style. Moreover, in order to obtain practical material properties, some specimens with same manufacturing process were tested. In order to perform the structural analysis, a finite element code, NISA II1), was used. In this analysis, linear static stress analysis, eigenvalue analysis and buckling analysis were carried out.

Finally, the structural design and safety of the designed blade was confirmed through the full-scale static structural test with the prototype blade made by hand lay-up manufacturing process.

2. Aerodynamic Design and Analysis

2.1 Theory[2]

According to the vortex theory of Glauert, the rotational speed of the wind flow relative to the blade rises to $\omega+\Omega$ at downstream of the rotor, and the angular velocity of the air flow in the plane of the rotor with respect to the blades can be expressed as,

$$\omega + \frac{\Omega}{2} = \left(\frac{1+h}{2}\right)\omega \tag{1}$$

where, Ω is increasing rotational angular speed vortices, ω is blade rotational angular speed, and h has the relationship of $(\omega+\Omega=h\omega)$. The axial speed through the rotor can be written as,

$$V = \frac{V_1 + V_2}{2} = \frac{1+k}{2} V_1 \tag{2}$$

where, V_1, V_2 are axial velocities at upstream and downstream of the plane of the rotor, and k is axial velocity ratio with the relationship of

$$(V_2 = kV_1).$$

Therefore the inclination angle and relative wind speed at a radius are then given in the rotor plane by the following equations.

$$\begin{cases} \cot I = \dfrac{U}{V} = \dfrac{\omega r}{V_1}\dfrac{1+h}{1+k} = \lambda\dfrac{1+h}{1+k} = \lambda_e \\ W = \dfrac{V_1(1+k)}{2\sin I} = \dfrac{\omega r(1+h)}{2\cos I} \end{cases} \tag{3}$$

where, U is blade rotational speed, λ is blade tip speed ratio and I is inclination angle in the rotor plane.

On the other hand, according to the blade elementary theory and the momentum theory, the blade aerodynamic load can be expressed as,

$$C_l b\, l = \frac{8\pi r(1-k)\sin^2 I\cos\varepsilon}{(1+k)\cos(I-\varepsilon)}$$
$$C_l b\, l = \frac{4\pi r(h-1)\sin 2I\cos\varepsilon}{(h+1)\sin(I-\varepsilon)} \quad (4)$$

where, C_l is lift coefficient of the used airfoil at radius r, b is number of blades, l is chord length and ε means $\tan^{-1}(C_d/C_l)$. And the local power coefficient at radius r can be expressed by the function of rotational angular speed ratio and axial velocity ratio as follows,

$$C_p \equiv \frac{dP_w}{\rho\pi r dr V_1^3} = \frac{\omega^2 r^2}{V_1^2}(1+k)(h-1)$$
$$= \lambda^2(1+k)(h-1) \quad (5)$$

In order to find rotational angular speed ratio and axial velocity ratio, the following relationship can be defined as,

$$G\equiv(1-k)/(1+k),\quad E\equiv(h-1)/(h+1)$$

If we use equation (3) and (4), the following relationship can be obtained.

$$\frac{G}{E} = \frac{(1-k)(h+1)}{(h-1)(1+k)} = \cot(I-\varepsilon)\cot I$$
$$= \frac{\lambda(h+1)+(1+k)\tan\varepsilon}{(1+k)-\lambda(1+h)\tan\varepsilon}\cdot\lambda\frac{1+h}{1+k} \quad (6)$$

Therefore the relationship between rotational angular speed ratio and axial velocity ratio can be finally expressed by,

$$h=\frac{-\tan\varepsilon+\sqrt{\tan^2\varepsilon+2\lambda k\tan\varepsilon+\lambda^2+(1-k^2)}}{\lambda} \quad (7)$$

If we find k_{opt} value to satisfy the condition of $dC_p/dk=0$ the optimum rotational angular speed ratio, inclination angle, blade load and local power coefficient can be calculated.

2.2 Characteristic of Airfoil

The blade airfoil configuration is an important factor to determine various performance parameters of the wind turbine system.

In this study, the airfoil of FFA-W3-211, which has relatively high stall angle of attack, maximum lift coefficient, maximum lift-drag ratio and very effective for structural strength due to relatively thick, was selected for the design purpose. Fig. 1 shows the airfoil configuration and aerodynamic characteristics[3].

2.3 Rated Wind Speed

The blade diameter of the wind turbine system can be approximately obtained from the equation (8) and (9) on the rated power. Fig. 2 shows variation of the blade radius depending on the rated wind speed. Here the blade radius is abruptly increased in case of designing below the rated wind speed of 6 m/s, but variation of the blade radius is small above the rated wind speed of 10 m/s. So we can obtain theoretical maximum power around this region. Therefore it is acceptable for keeping adequate length at the low wind speed when the rated wind speed to decide the blade radius is determined at 8 m/s.

$$P_{max} = 0.37 A V^3 \quad (8)$$

where, P_{max} is maximum power by Betz theory, A is Swept area and V is Rated wind speed. Therefore, we can obtain the following relationship to determine the blade diameter, approximately.

$$P = 0.2 D^2 V^3 \quad (9)$$

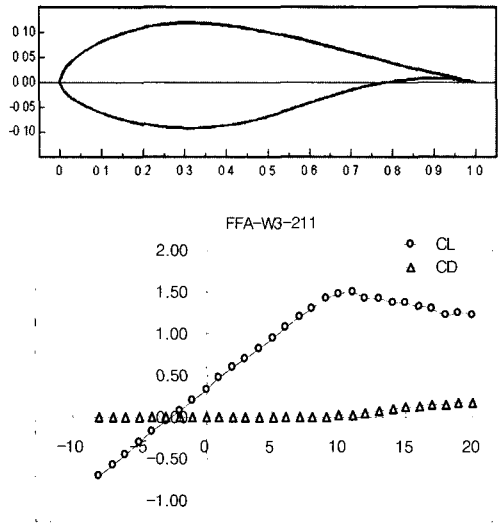

Fig. 1 Airfoil shape and aerodynamic characteristics of FFA-W3-211

2.4 Blade Design

There are several methods to design aerodynamically the blade such as chord length and twist angle.

In this study, two methods, which are the most general method to find the optimum inclination angle with maximum lift-drag ratio and the method to get the linear chord length distribution, were investigated. Fig. 3 shows comparison between design results using maximum inclination angle design method and them using the linear chord length distribution method with the taper ratio of 0.3. Fig. 4 shows variation of power coefficients by two methods. From the Fig. 3, it was found that the maximum inclination angle design method was more effective method because of reduction of the chord length. Specification of the finally designed blade is shown in Table 1. Fig. 5 shows the designed aerodynamic configuration.

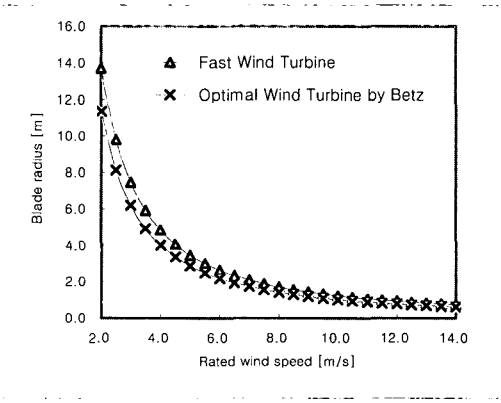

Fig. 2 Rated wind speed vs blade radius

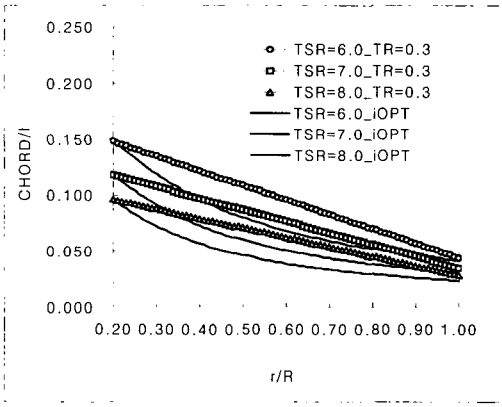

Fig. 3 Distribution of the chord

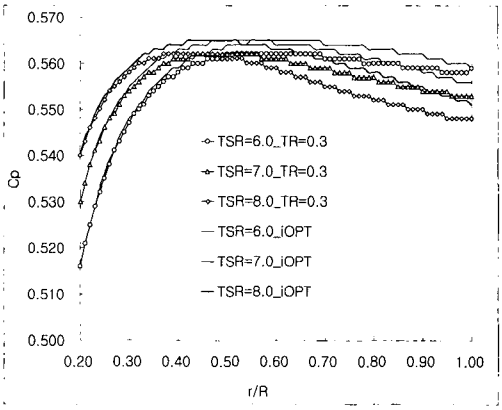

Fig. 4 Local power coefficient

Table 1. Aerodynamic design results

Rated power	1 kW
Cut in wind speed	3.0 m/s
Rated wind speed	8.0 m/s
Cut out wind speed	25 m/s
Design tip speed ratio	6.0
Rated RPM	268 rpm
Number of Blades	3
Rotor diameter	3.42 m
Aerodynamic profile	FFA-W3-211
Blade root chord	253 mm
Blade tip chord	73 mm
Blade total twist	20.23 deg.

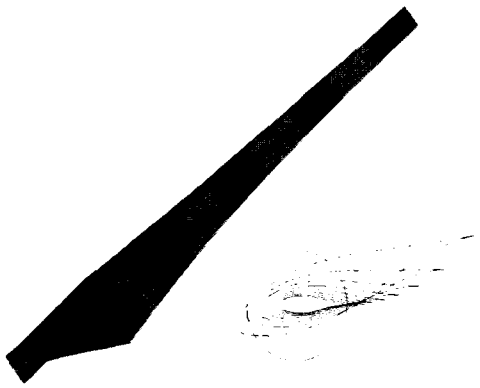

Fig. 5 Designed aerodynamic shape of 1kW class wind turbine blade

2.5 Aerodynamic Analysis

Figure 6 shows power variation at each wind speed depending on the blade rotational speed. In this figure, we can find the specific rotational speed with maximum power at each wind speed. Fig. 7 shows power variation versus wind speed variation at optimum rotational speed.

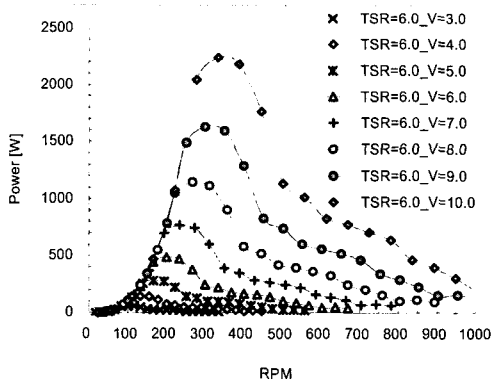

Fig. 6 Aerodynamic power vs. RPM

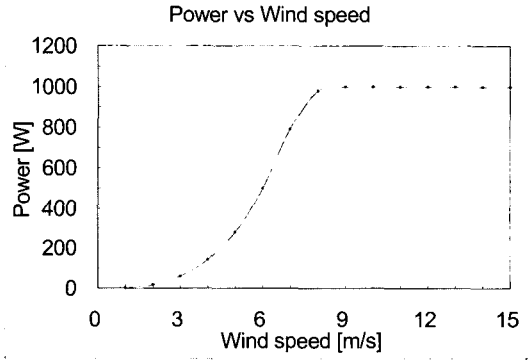

Fig. 7 Aerodynamic power vs. wind speed

3. Structural Design and Analysis

3.1 Structural Design

3.1.1 Design Load

Loads acted on the wind turbine blade are divided into major aerodynamic loads and subsidiary loads due to gravity, motion and centrifugal force in rotating, ice, temperature and humidity effects, faults of the wind turbine system, braking, etc. It is very difficult to analysis all these loads because they are inter-related to each other. Therefore, the aerodynamic loads mainly acted on the blade are analyzed here. Table 2

shows the load cases for the blade design. The maximum load case is the load case II, that is the rated wind speed condition with the gust wind and variation of the wind direction. Therefore, the structural design was carried out based on the load case II. Fig. 8 shows the flap-wise moment distribution of the design load case.

Table 2. Load case for structural design

Load Case	Case I	Case II	Case III
Reference wind speed	8.0 m/s	25.0 m/s	55.0 m/s
Gust condition (±20 m/s, ±40 deg)	Without gust	With gust	Storm condition
Rotational speed	268 rpm	300 rpm	Stop

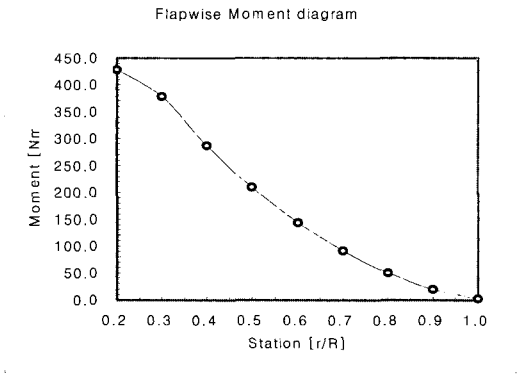

Fig. 8 Flap-wise moment diagram for load case II

Figure 9 shows the representative sectional view of the blade structure. The bending force is endured by spar flange layered in the ply angle (0°/90°) with E-Glass/Epoxy fabric. The torsion moment is kept by upper and lower skin layered in the ply angle (45°) with E-Glass/Epoxy fabric. In order to reduce the weight and to strengthen both the dynamic stability and the buckling strength, the sandwich structure with the urethane foam core was used. Moreover, the compression side spar is slightly thicker than the tension side spar. The main spar flange is extended to the tip of the blade, but its thickness is gradually reduced along the spar to reduce the weight. The structural configuration for the rotor blade is determined by trial and error. Table 3 shows the sectional thickness for the skin and the spar flange of upper and lower blade parts.

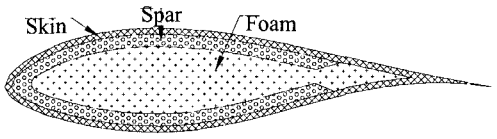

Fig. 9 Section view of the blade structure

Table 3. Structural design results

Station (r/R)	Thickness(mm)	
	Upper surface	Lower surface
Root~0.1	10t/Skin 1.25t /Spar 7.00t(AL2024)	
0.1~0.2	Skin 1.25t/Spar 4.75t	Skin 1.25t/Spar 3.00t
0.2~0.3	Skin 1.25t/Spar 3.75t	Skin 1.25t/Spar 2.25t
0.3~0.4	Skin 1.25t /Spar 3.50t	Skin 1.25t/Spar 2.00t
0.4~0.5	Skin 1.25t /Spar 3.25t	Skin 1.25t/Spar 1.75t
0.5~0.6	Skin 1.25t /Spar 3.00t	Skin 1.25t/Spar 1.50t
0.6~0.7	Skin 1.25t /Spar 2.50t	Skin 1.25t/Spar 1.25t
0.7~0.8	Skin 1.25t /Spar 2.00t	Skin 1.25t/Spar 1.00t
0.8~0.9	Skin 1.25t /Spar 1.50t	Skin 1.25t/Spar 0.75t
0.9~Tip	Skin 1.25t /Spar 0.75t	Skin 1.25t/Spar 0.50t

3.1.2 Specimen Test

Generally, the strength of the open mold composite is lower than it of the autoclave mold composite. Most literature data of

composite materials are based on the autoclave molded specimen test. Therefore the specimen tests for open molded glass/epoxy composite should be requested. Fig. 10 shows the test specimen and Table 4 shows the specimen test results.

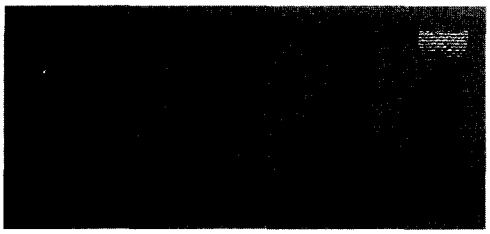

Fig. 10(a) Compression test specimen [ASTM D695]

Fig. 10(b) Tensile test specimen [ASTM D638]

Table 4. Mechanical properties of materials used in the present blades design

Material / Property	Glass/Epoxy Fabric	Polyurethane Foam
E1 (N/mm2)	10500	60.86
E2 (N/mm2)	10500	59.86
G12 (N/mm2)	1450	19.18
ν	0.27	0.2
Xt (N/mm2)	283.9	2.63
Xc (N/mm2)	184.6	1.41
Yt (N/mm2)	283.9	2.49
Yc (N/mm2)	184.6	1.41
S (N/mm2)	15.0	0.71
S (N/mm2)	1.705	0.1197
Ply thickness (mm)	0.25	12.5

3.2 Structural Analysis

The finite element program used for structural analysis is a commercial code NISA II and the post-processing program for displaying the output is DISPLAY III. The element types used for the analysis are the 3-D composite shell element and the number of total elements is 960. Generally, failure is governed by directional material strengths rather than principal stress or strains. Intra-lamina failure criterion used for this design are both the Maximum Stress Failure Criterion[5] and the Tasi-Wu failure criterion[6].

3.2.1 Linear static analysis

According to analysis results, the total weight of the blade is calculated to be 3.16 kg. By the failure criterion the minimum safety factor was 2.6 and confirmed safe. Table 5 shows the stress analyses results for three load cases. Fig. 11 shows the stress distribution at the first ply of the spar flange for the load case II.

3.2.2 Eigenvalue analysis

Dynamic effects can be substantial in a wind turbine system because of the periodic nature of its aerodynamic loading. As a result, the design process must depend on determination of the dynamic characteristics of the rotating structure. In this study, modal analysis is performed by the finite element method. Fig. 12 shows the results of modal analysis for natural frequencies such as the first flap-wise and chord-wise bending modes, displayed in a frequency plot so called a Campbell diagram. Rays of origin are plots of integer multiples of the rotational frequency. In a rotating structure, excitation

loading occurs normally at these multiple frequencies, often abbreviated 1p(once per rotation), 3p, 6p, etc. Resonance is a phenomenon, which occurs in a structure when the frequency of periodic loading or excitation equals or nearly equals one of the modal frequencies of the structure. Thus, as shown in Fig. 12, because there are no intersections of a radial line and a modal frequency line, there may not be any resonance between the blade and excitation loadings. Fig. 13 shows the first flap-wise mode shape and frequency.

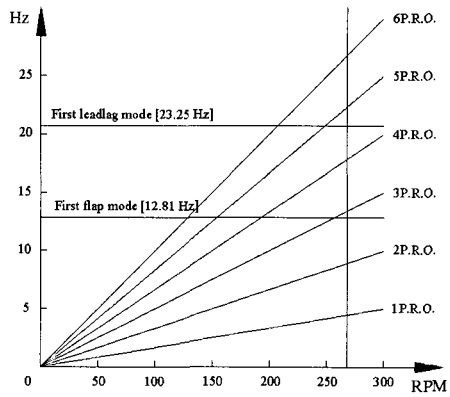

Fig. 12 Campbell diagram

Table 5. Structural analysis result

Case of Analysis / Analysis Result		Case I	Case II	Case III
Max. Stress [Mpa]	Ten.	13.9	38.5	33.3
	Com.	10.8	31.1	29.4
Max. Disp. [mm]		52.84	**151.0**	123.2
Max. stress failure critrion	Sxx/allow	0.053	0.165	0.162
	Syy/allow	0.027	0.089	0.095
	Sxy/allow	0.125	**0.384**	0.364
Tsai-Wu failure critrion		0.035	0.217	0.205

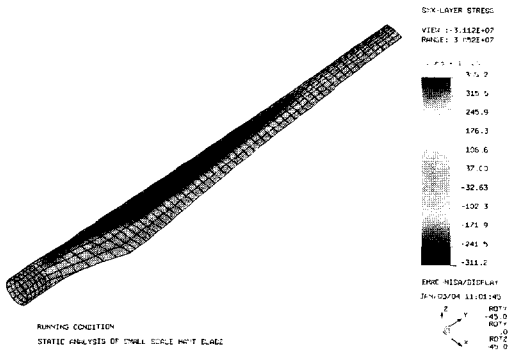

Fig. 11 Stress analysis result of load case II

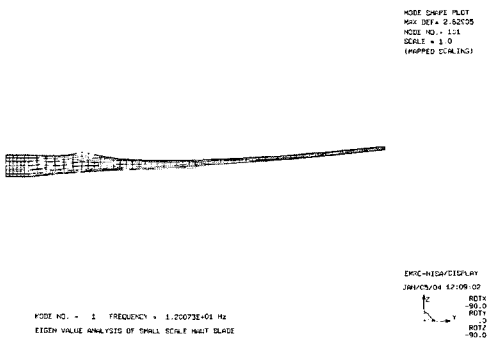

Fig. 13 First flap mode shape and frequency

3.2.3 Buckling analysis

Because the thin walled structure like a wind turbine rotor blade studied here may have structural instability such as buckling, the structural stability under compressive loading and shear loading should be checked. In this study, the buckling analysis is done by the finite element method. The finite element modeling for buckling analysis is the same as the static analysis modeling under loading the load case II. Fig. 14 shows buckling load factors for the first buckling mode and buckling location of the blade. The buckling load factor means the ratio of the buckling load to the applied load. Generally, the most important

buckling mode is the first mode, i.e. the critical mode. In this study the minimum buckling load factor was 2.18 and confirmed safe.

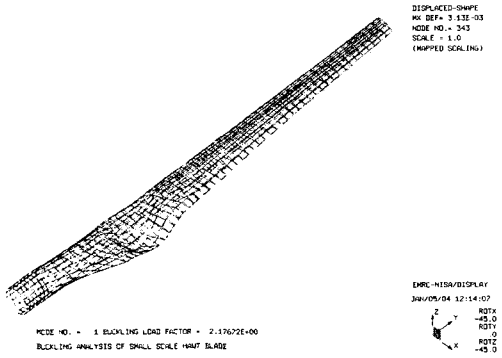

Fig. 14 First buckling mode shape and load factor

4. Full Scale Structural test

4.1 Eigenvalue Test

In order to measure the natural frequency of the blade, it was impacted by impulse hammer, and the strain values were acquired by AI1600 of SASCO data acquisition system. At measurement of data, the sampling frequency was 500 Hz. The Fast Fourier Transforms(FFT) of the obtained strain data were performed by MATLABR program. Fig. 15 shows the obtained strain data and the FFT analysis results. Table 6 shows the measured and predicted natural frequency. As shown in the table, the predicted values are in good agreement with the measured values.

Table 6. Comparison between measured and predicted natural frequency

Mode shape	Analysis resusts	Test results
First Flap Mode	12.81 Hz	11.72 Hz
First Leadlag Mode	23.25 Hz	21.09 Hz
Second Flap Mode	42.77 Hz	41.31 Hz

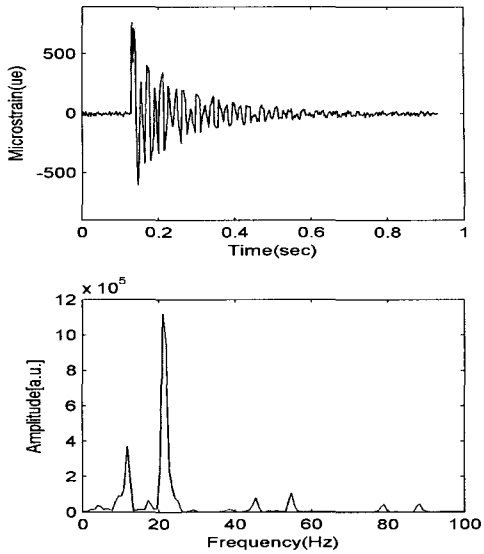

Fig. 15 Eigenvalue test result

4.2 Static Strength Test

The manufactured prototype blade was set on the test rig and loaded at 0.9m, 1.2m and 1.6m stations of the blade, and strains and deflections of the blade were measured. As a load for the static test, the load case II was used. The load case II has the aerodynamic load at the cutout wind speed in practical operation including gust. In order to simulate the aerodynamic load, the three-point loading method is applied. Fig. 16 shows load values and loading points in flap-wise direction for the static strength test.

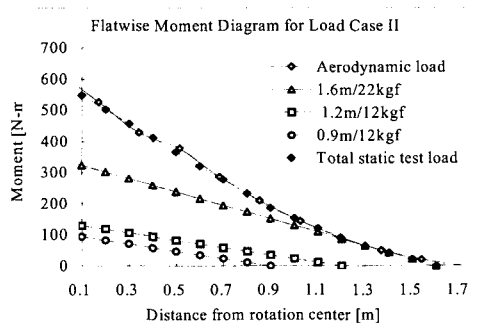

Fig. 16 Static strength test loads simulated by three-point loading method

A prototype blade for the static strength test was tested, and used for comparison with the analyzed model. During the test up to the maximum loading, there was no failure such as catastrophic failure, local failure, de-bonding, de-lamination, local buckling, etc. Table 7 shows both measured and predicted results for stresses on the upper and lower surface of the 0.2 r/R station and the tip defection. Prediction was in good agreement with the measured values indicating that, at least, the physical construction of the blade was modeled reasonably well. Fig. 17 shows the loaded blade and three-point loadings by sandbag.

Table 7. Comparison between the linear static analysis results and the static test results

Item	Analysis results	Test results
Tip displacement	131 mm	150 mm
Upper and lower surface stresses at 0.2 r/R station	+29.7 Mpa -21.8 Mpa	+27.0 Mpa -16.9 Mpa

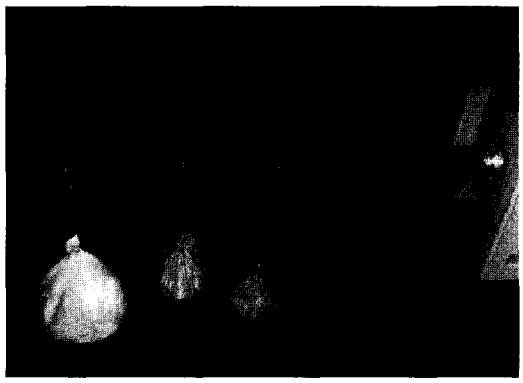

Fig. 17 Static test of the prototype blade

5. Conclusion

Through the present study, the optimum aerodynamic configuration of the small wind turbine blade was proposed by parametric studies. From the results of the aerodynamic design, the designed blade has about 1kW power at the rated wind speed of 8 m/s. It is more efficient at low wind speed and its diameter is not much larger than similar class other blades. In structural design, a light composite structure, which can endure effectively various loads, was designed. In order to evaluate the designed structure, the structural analysis was performed by the finite element method. According to linear static structural analysis, it was confirmed that the safety of the structure had about 2.6 at the maximum operation wind speed of 25 m/s. In order to keep the safety for the extreme condition, it was analyzed in storm condition with wind speed of 55m/s. In this analysis, it was confirmed the safety factor of 2.75. In case of the eigenvalue analysis, it was obtained that the natural frequencies were the 1st flap mode of 12.81 Hz and the 1st lead-lag mode of 23.25 Hz. It was found that the blade had no resonance in operating range. For the buckling analysis, it had a sufficient buckling load factor of 2.18 by using the foam sandwich structure. The full-scale static structural test was performed under the simulated aerodynamic loads. From the experimental results, it was found that the designed blade had the structural integrity. Furthermore the measured results were well agreed with the analytical results such as deflections, strains and natural frequency.

eferences

1. EMRC, NISAII-Users Manual, Version5.2, 1992
2. D. LE Gourieres, Wind power plants, Pergamon Press, 1982, pp.75-101
3. Frank, B. et al., Wind turbine airfoil catalogue, Riso national laboratory, 2001, pp.81-84
4. Kong, C. et al., Structural Design of Medium Scale Composite Wind Turbine Blade, 13th International Conference on Composite Materials (ICCM-13), 2001, pp. 561
5. Gibson, R. F., Principles of composite material mechanics, McGraw-Hill, Inc., 1994, pp103-106
6. Feng, W. A failure criterion for composite materials, Journal of composite materials, 25(1), 1991, pp.88-100